

PAPER • OPEN ACCESS

Large reciprocal magneto-optical effect induced by all-dielectric resonant gratings based on a magnetic nanocomposite

To cite this article: Laure Bsawmaï *et al* 2023 *New J. Phys.* **25** 063021

View the [article online](#) for updates and enhancements.

You may also like

- [The 2022 magneto-optics roadmap](#)
Alexey Kimel, Anatoly Zvezdin, Sangeeta Sharma *et al.*
- [Optical nonreciprocal devices based on magneto-optical phase shift in silicon photonics](#)
Y Shoji, K Miura and T Mizumoto
- [Magnetorheological elastomers with particle chain orientation: modelling and experiments](#)
Jianfei Yao, Wei Yang, Yu Gao *et al.*



PAPER

Large reciprocal magneto-optical effect induced by all-dielectric resonant gratings based on a magnetic nanocomposite

OPEN ACCESS

RECEIVED

20 October 2022

REVISED

15 May 2023

ACCEPTED FOR PUBLICATION

13 June 2023

PUBLISHED

23 June 2023

Original Content from
this work may be used
under the terms of the
[Creative Commons
Attribution 4.0 licence](https://creativecommons.org/licenses/by/4.0/).

Any further distribution
of this work must
maintain attribution to
the author(s) and the title
of the work, journal
citation and DOI.

Laure Bsawmaï¹ , Emilie Gamet¹ , Yaya Lefkir¹, Sophie Neveu², Damien Jamon¹ and François Royer^{1,*} ¹ Université de Lyon, CNRS, UMR 5516, Institut d'optique Graduate School, Laboratoire Hubert Curien, Université Jean Monnet, 18 rue Pr. Laurus, F-42000 Saint-Etienne, France² Sorbonne Universités, CNRS, Laboratoire PHENIX, UMR 8234, F-75005 Paris, France

* Author to whom any correspondence should be addressed.

E-mail: francois.royer@univ-st-etienne.fr**Keywords:** enhanced magneto-optics, all-dielectric resonant gratings, magneto-induced anisotropy, reciprocal effects**Abstract**

The beneficial combination of micro- and nano-patterned surfaces with magneto-optical materials was investigated over the recent years. Due to their resonant behavior, these structures are commonly used to enhance the non-reciprocal magneto-optical effects. In this paper, a novel kind of magneto-optical intensity effect is enhanced with an all-dielectric grating patterned on a magnetic nanocomposite layer. This nanocomposite is made of CoFe_2O_4 nanoparticles (NPs) embedded in a silica matrix by sol-gel technique. The demonstrated magneto-optical intensity effect is reciprocal and it is observed with transverse magnetic field, for both polarization (TE and TM) and small angles of incidence. Such effect is not explained by the classical appearance of off-diagonal elements in the permittivity tensor of the magneto-optical material under magnetic field. However, it can be attributed to a magneto-induced reciprocal modification of the diagonal elements. Furthermore, this effect strongly depends on the NPs orientation inside the magneto-optical film and can originate from the magnetostrictive property of the magnetic CoFe_2O_4 NPs.

1. Introduction

From several years, the enhancement of magneto-optical (MO) effects is taking lots of attention due to their sensitivity to the magnetic field, their fast modulation of light [1] and their potential in enhancing the sensitivity of biosensors [2, 3]. These effects [4] are described as a rotation of the polarization plane or a modulation of the intensity, of the reflected or transmitted light through a magnetized material.

The development over the recent decades of micro- and nano-patterned surfaces [5–7] opened the field to the exploration of several optical phenomena. Combining these surfaces with MO materials enhances drastically the MO effects. Indeed, the excitation of optical modes (plasmonic [8] or dielectric [9]) in the micro and nano-structures produces resonances in optical transmittance or reflectance spectra. Due to the MO material, the polarization and dispersion of these modes can be tuned by the magnetic field, resulting hence in resonances in the MO effect spectra. In particular, for the case of magnetization directed in-plane and perpendicular to the mode propagation [10], the guided transverse MO Kerr effect (TMOKE) induces a modulation of the propagation constant or the extinction coefficient of the TM guided-mode for planar waveguides. In the resonant structures, this effect manifests as a spectral shift or amplitude variation of the transmittance (reflectance) resonance, resulting in a resonant intensity modulation of the transmitted (reflected) light. Hence, the TMOKE is defined as the relative change of the intensity I of the transmitted (or reflected) light upon magnetization M reversal [11]:

$$\text{TMOKE (\%)} = 100 \times \frac{I(+M) - I(-M)}{\frac{1}{2}(I(+M) + I(-M))}. \quad (1)$$

Different resonant structures have been implemented to enhance the TMOKE, but also Faraday or longitudinal rotation, such as Au/Co heterostructures [3, 12–14] or perforated Au layer deposited on top of a dielectric magnetic film (generally Bismuth Iron Garnet) [8, 15, 16] as well as dielectric gratings with MO composite material [17–19]. The effects described above are non-reciprocal, and thus induce a MO response which is odd as a function of the magnetic field [19]. Indeed, when a magnetic field is applied, a skew-symmetric coupling between the electric field components is created resulting in off-diagonal elements of the material permittivity tensor [4]. An example of the permittivity when a magnetic field is applied following z direction, is described as follows:

$$\begin{pmatrix} \epsilon_{xx} & i\epsilon_{xy} & 0 \\ -i\epsilon_{xy} & \epsilon_{yy} & 0 \\ 0 & 0 & \epsilon_{zz} \end{pmatrix}. \quad (2)$$

The ϵ_{xy} term is proportional to the magnetization directed along z . In non-reciprocal case, the MO effect is proportional to ϵ_{xy} .

Apart from the non-reciprocal effects (REs) there are some reciprocal MO intensity effects (even as a function of the magnetic field): Cotton Mouton [4], MO orientational effect [20], magnetorefractive effect [21], magnetostrictive [22], etc. These effects are much less known mainly because of their smaller magnitudes [23], e.g. the Cotton Mouton effect, in magnetic thin films, is smaller by three orders of magnitudes than the TMOKE.

Nevertheless, Belotelov *et al* [24], demonstrated an experimental and theoretical enhancement of a reciprocal intensity modulation effect, in longitudinal configuration and at normal incidence, through a resonant structure. This latter consists of a gold grating deposited on top of a Bi:YIG film. The origin of this RE is explained as follows [25]: due to the longitudinal applied magnetic field, the guided-modes (Transverse Electric/TE or Transverse Magnetic/TM) excited in the MO layer transform into quasi-modes with additional field components that vary linearly with respect to the MO term ϵ_{xy} . Thus TE modes that are dark for TM incident light become bright quasi-TE modes. This linear change produces quadratic change in transmittance.

In the presented work, another kind of reciprocal modulation intensity effect is investigated. It was observed with an all-dielectric resonant device based on a MO nanocomposite material with a transverse magnetic field. This effect, called transverse reciprocal effect (TRE), is defined as the relative change of the transmitted (or reflected) intensity I , between the magnetized $\left(\frac{I(+M)+I(-M)}{2}\right)$ and demagnetized $I(0)$ structure:

$$\text{TRE (\%)} = 100 \times \left(\frac{I(+M) + I(-M)}{2I(0)} - 1 \right). \quad (3)$$

2. Material and methods

The structure under consideration is illustrated in figure 1(a) and consists of a dielectric grating patterned on top of a MO composite film deposited on a glass substrate. The MO composite [26–28] consists of magnetic nanoparticles (NPs) embedded in a silica matrix through a sol–gel process.

Such MO material is obtained from a liquid sol–gel preparation of Tetraethyl Orthosilicate ($\text{Si}(\text{OC}_2\text{H}_5)_4/\text{TEOS}$) doped with magnetic NPs. To manage such doping, a ferrofluid made of Cobalt Ferrite (CoFe_2O_4) NPs dispersed in water is introduced in the sol–gel preparation. The added quantity of ferrofluid drives the volume fraction of NPs in the final nanocomposite and defines the MO activity as well as the refractive index of the material [18].

This MO material is then deposited on top of a glass substrate by dip-coating followed by an annealing at 90°C during one hour in order to eliminate the persistent solvents and start the densification process of the MO composite.

In order to further study the effect of the NPs orientation in the MO composite, different MO films were deposited under magnetic field (denoted \vec{B}_{gel}) with different orientations with respect to the film plane (see figure 1(a)). During dip coating, the NPs magnetic moments ($\vec{\mu}$) tend to align along the gelation magnetic field. Once the film is dry, the NPs are prevented from moving in the solid matrix [26]. As CoFe_2O_4 NPs are both optically and magnetically anisotropic, the gelation magnetic field has two consequences: a permanent optical anisotropy is created which optical axis (\vec{n}) is parallel to the direction of \vec{B}_{gel} , and the magnetic behavior of the composite is modified with an easy axis of magnetization also aligned with \vec{B}_{gel} . For more details the readers are invited to consult [28]. Table 1 summarizes the different fabricated MO films.

The measurements of the in-plane permanent anisotropy ($\Delta n = n_x - n_z$) for the MO films deposited under in-plane gelation field are plotted on figure 1(b) as a function of the wavelength. The measurements

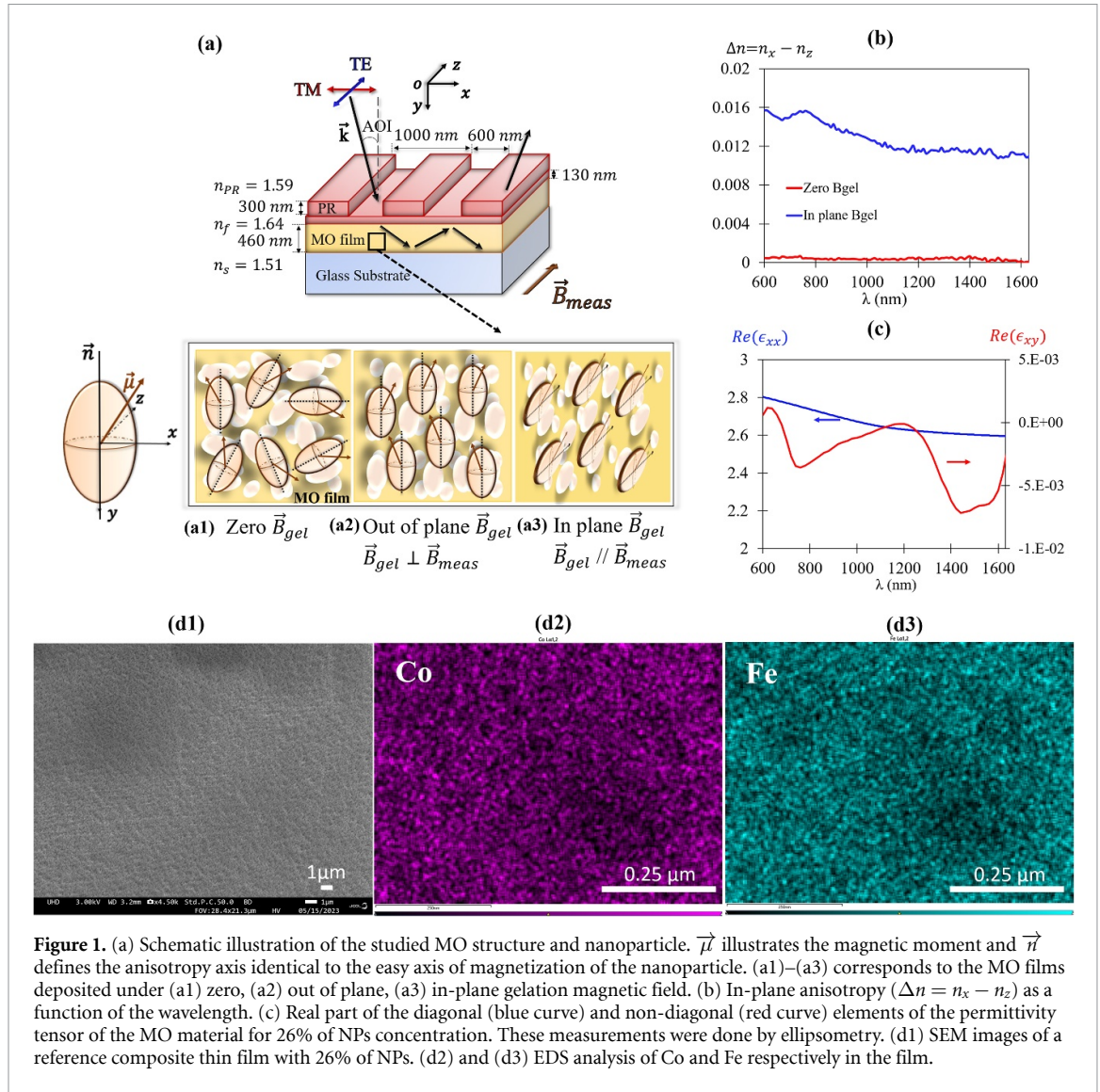


Table 1. The fabricated MO films with the corresponding orientation of the gelation magnetic field.

MO structures	Magnetic field (\vec{B}_{gel}) orientation
a1	Zero field
a2	Out of plane
a3	In-plane

were done by ellipsometry in transmission. As seen in this figure, the amplitude of the permanent anisotropy is more important in the visible region than in the near IR, which is related to the refractive index dispersion of the NP. The permanent anisotropy reaches a value of $\Delta n = 10^{-2}$ around $\lambda = 1550$ nm.

Then, a photoresist 1D grating was patterned on top of the different MO films to obtain the resonant structures. Such dielectric grating was obtained by patterning a positive photoresist (S1805©) film using a classical photolithographic manual machine based on a Mercury vapor lamp ($\lambda = 360$ nm) and a periodic quartz-supported chromium mask.

The association of such a grating to the guiding MO layer induces a guided-mode resonant behavior, and the device produces peaks of reflectance spectrum (or dips of transmittance) for TE and TM polarization at the resonance wavelength. Such resonance condition is written through [29]:

$$\beta = 2\pi \sin(\text{AOI})/\lambda_0 + 2m\pi/\Lambda. \quad (4)$$

β is the propagation constant, λ_0 is the resonance wavelength, AOI is the angle of incidence, m is the diffraction order and Λ is the grating period.

To obtain a resonance around $\lambda = 1550$ nm with the given refractive indices (see figure 1(a)) and small angles of incidence (AOI), the period of the mask was fixed at 1000 nm.

The MO effects were measured employing a homemade MO setup. It consists mainly of a light source, a linear polarizer mounted on a rotating support with 0.001° of resolution, an electromagnet and a photodetector. The source is a laser DL pro TOPTICA photonics. Its wavelength can be tuned manually (1490 nm–1630 nm) and measured with an Optical Spectrum Analyzer (OSA-HP 70950B). The polarizer is used to fix the polarization of the light impinging on the sample, in other words, it serves to choose between TE and TM polarization. The electromagnet generates a magnetic field (\vec{B}_{meas}) with an amplitude that can reach ± 900 mT thanks to a 4 quadrant linear amplifier HUBERT 1110-16-QE. The sample is fixed between the pole pieces of the electromagnet by a vacuum sample holder, mounted on a motorized rotating support with five axes (PRMTZ8/M THORLABS). The intensity of the reflected light is finally measured with the photodetector (New FocusTM) for each wavelength.

The TRE and TMOKE measurements consist in varying continuously the magnetic field for a fixed wavelength, and simultaneously measured the intensity of the reflected light with the photodetector. As a result, an intensity hysteresis loop (see figure 2(a)) is obtained for each wavelength. The TMOKE is then deduced from opposite saturated intensity values using (1) and then plotted as a function of the wavelength. The TRE is also deduced from these values but employing (3).

Optical and MO simulations were performed on the basis of the rigorous coupled waves analysis (RCWA) method, extended to the case of MO materials taking into account the permittivity tensor in the form of (2).

The material parameters of the MO composite, used in the RCWA simulations are $\epsilon_{xx} = (n - ik)^2 = 2.59 - i0.014$ and $\epsilon_{xy}(M) = -0.0064 + i0.0044$ at $\lambda = 1550$ nm, for a saturated field of 900 mT (ϵ_{xy} is fixed to zero for $M = 0$). The value of ϵ_{xy} of the composite material was calculated using the relation between the Faraday effect and complex off-diagonal elements given in [30], applied to data obtained through the measurements of the Faraday effect (rotation and ellipticity), and the complex refractive index of a reference sample consisting of a composite thin film with 26% of NP, without any grating.

For out-of plane sample, the measured permanent optical anisotropy (Δn , see figure 1(b)) was added to ϵ_{yy} , even in the absence of an applied magnetic field. Hence, the permittivity tensor used in the numerical simulations for out-of plane gelation sample with an applied magnetic field is defined as follows:

$$\epsilon(M, \lambda) = \begin{pmatrix} \epsilon_{xx}(0) = (n - ik)^2 & i\epsilon_{xy}(M, \lambda) & 0 \\ -i\epsilon_{xy}(M, \lambda) & \epsilon_{yy}(0) = (n + \Delta n - ik)^2 & 0 \\ 0 & 0 & \epsilon_{zz}(0) = (n - ik)^2 \end{pmatrix}. \quad (5)$$

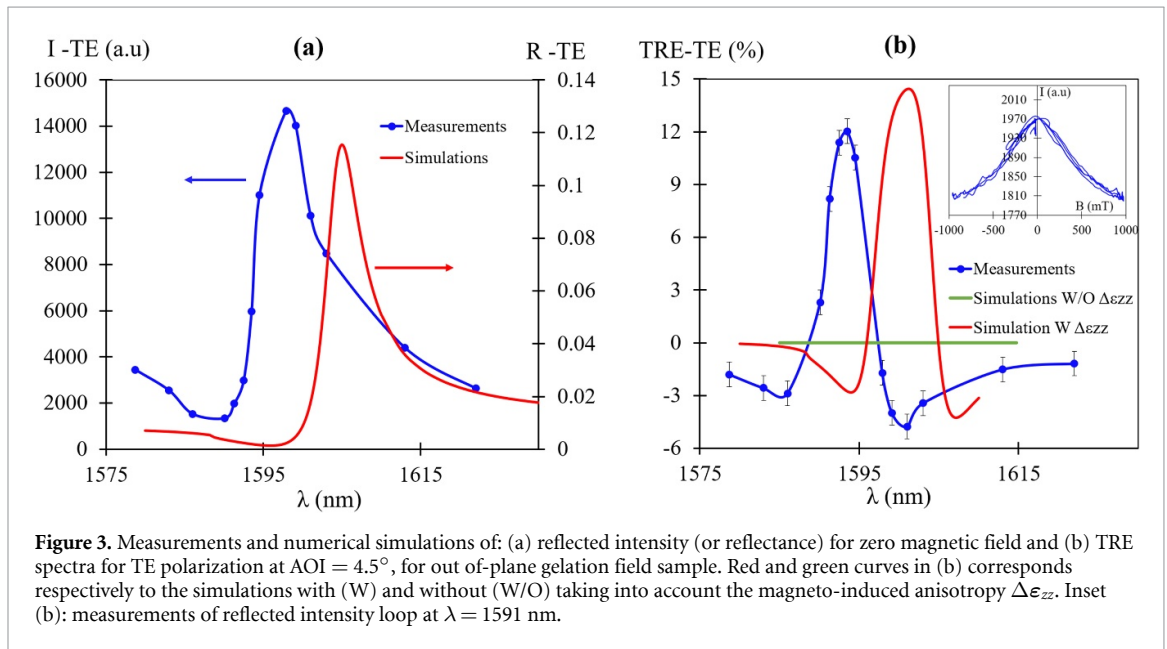
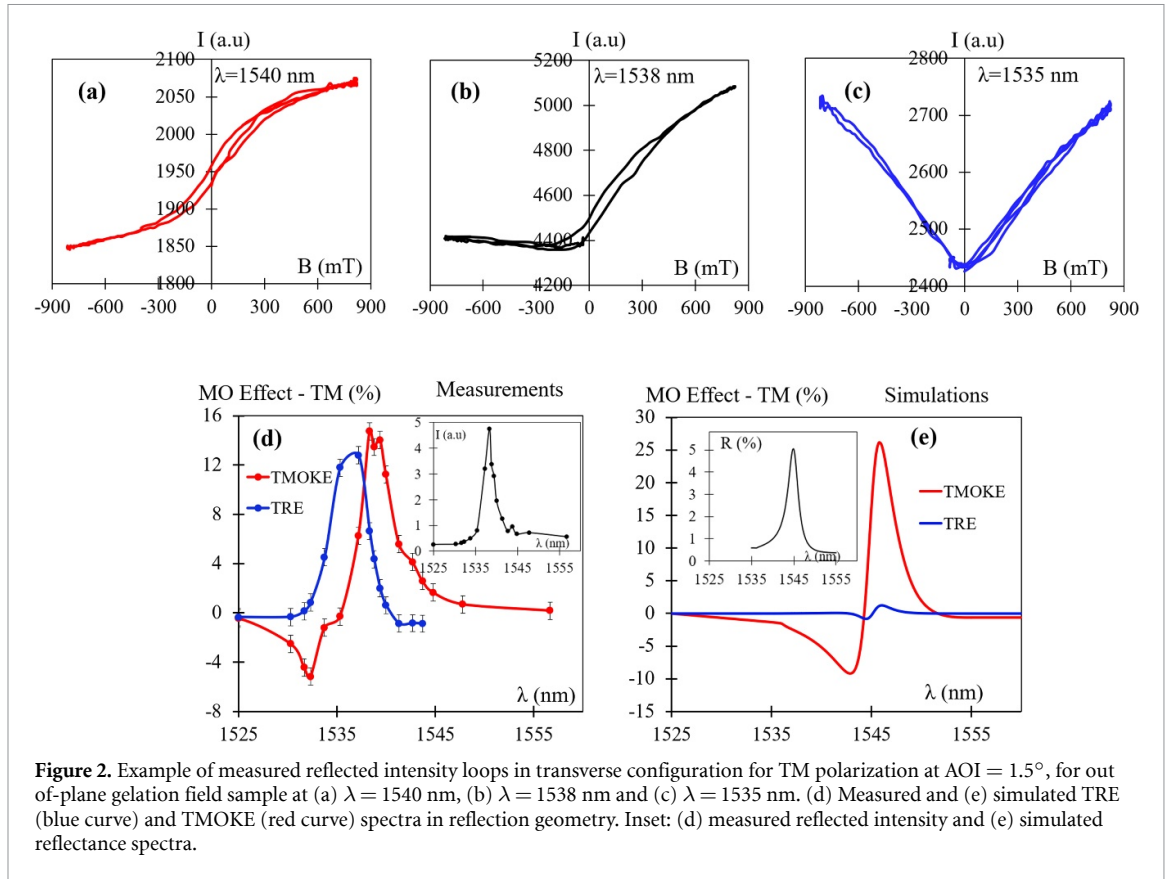
The dispersion of the non-diagonal elements is taken into consideration, however the diagonal part is fixed in the range of (1490 nm; 1630 nm) due to its non dispersive behavior in such a reduced spectral range (see figure 1(c)). The photoresist grating and the glass substrate are modeled with a constant permittivity equal to 2.53 and 2.28, respectively.

3. Results and discussion

Figures 2(a)–(c) illustrates different intensity hysteresis loops at different wavelengths, in transverse configuration (\vec{B}_{meas} following z direction in figure 1(a)) and in reflection. The polarization of the incident light is TM (electric field in x direction) and the AOI is equal to 1.5° . As seen in figures 2(a)–(c) the curve is odd in magnetic field at $\lambda = 1540$ nm (red curve), whereas it is even at 1535 nm (blue curve). At 1538 nm (black curve), the behavior is a mix of the two previous situations. Hence, in addition to the non-RE (TMOKE) a RE is clearly evidenced: the curve is no more odd as a function of the field.

This is confirmed by the TRE and the TMOKE experimental spectra (blue curves) illustrated in figure 2(d), which shows that at $\lambda = 1535$ nm the TMOKE is weak (TMOKE = -0.3%) and the TRE is very high (TRE = 12%) resulting in a symmetric intensity loop (figure 2(c)). However, at $\lambda = 1540$ nm, the TMOKE is very high (11%) compared to the TRE (0.6%), resulting in an antisymmetric curve (figure 2(a)).

One can notice also from figures 2(d) and (e), that the maximum measured TRE value (13%) is one order higher than the simulated one (1.2%). Such difference demonstrates that the simulations do not explain the measured TRE. As explained before, in these simulations, the influence of the magnetic field on the MO material properties is uniquely taken into account through the modification of the off-diagonal elements ϵ_{xy} (referring to (5)). No modification of the diagonal part due to the magnetic field is considered, as it is classically led for MO material. Therefore, we can deduce that the high measured TRE is the sum of the effect considered by the simulations that can be attributed to enhanced Cotton Mouton [4] effect, plus another effect which origin will be discussed in this paper. It is worth noticing on figure 2(e) that the



difference between the simulations (26%) and the measurements (15%) of TMOKE values can be attributed to the emission spectral width of the laser (light source used in the experimental setup) that has a larger full width at half maximum (FWHM) than the TMOKE resonance FWHM. Thus, the measured TMOKE value is averaged over this spectral range, decreasing hence the real maximum value of the TMOKE signal (the readers are invited to consult [19] for a full analysis of TMOKE).

The TRE in reflection was also studied for TE polarization at AOI = 4.5°. Figures 3(a) and (b) illustrates the measurements and numerical simulations of reflected intensity (or reflectance) and TRE spectra. In this case, the intensity loop is totally symmetric for each wavelength, since there is no TMOKE for TE polarization [4] (see inset figure 3(b)). As seen in this figure, the measured TRE (blue curve) reaches a

maximum value of 12% at $\lambda = 1593.5$ nm. For the numerical simulations (figure 3(b), green curve), the TRE is zero when the classical form of the permittivity tensor is taken into account (see (5)).

It is worth noticing on figure 3(a), a spectral shift between the experimental (blue curve) and numerical (red curve) spectra. This difference can be related to the imperfections of the fabricated structures (height, thicknesses, etc) and to the reading of the AOI. Indeed, we used a manual goniometer to read the AOI resulting in a small reading error ($\approx 0.25^\circ$). This error may shift the experimental resonant wavelength from the numerical one, according to the coupling grating equation (see (4)).

In order to study and understand the origin of such high measured values of TRE, numerical simulations have been carried out, taking into account an induced optical anisotropy in z direction under magnetic field. The chosen direction of the magneto-induced optical anisotropy is related to the direction of the applied magnetic field (\vec{B}_{meas}) which is here following z direction. Hence, a variation is added to the diagonal part of the material permittivity tensor (see (6)), under magnetic field: $\epsilon_{zz}(M) = \epsilon_{zz}(0) + \Delta\epsilon_{zz}$. The calculated spectra are illustrated in figure 3(b) (red curve). One can see, that these simulations are very consistent with the experimental measurements (figure 3(b), blue curve) in term of amplitude as well as spectral behavior. Different values of $\Delta\epsilon_{zz}$ have been used in the calculation code and the closest simulated spectrum (in term of amplitude) to the experimental one corresponds to $\Delta\epsilon_{zz} = -1.64 \times 10^{-3}$ (figure 3(a)).

It is important to mention that other numerical simulations were carried out taking into account additional optical anisotropies (in x and y directions) under magnetic field. However, the results confirm that only the induced optical anisotropy in z direction ($\Delta\epsilon_{zz}$) can explain the TRE observed in the TE experimental measurements of figure 3(b). In other words, in that case the numerical simulations are exactly the same with or without adding $\Delta\epsilon_{xx}$ or $\Delta\epsilon_{yy}$ under magnetic field. It is in agreement with the fact that the propagation constant of the TE mode, β_{TE} , only depends on ϵ_{zz} in such anisotropic guiding layer. Thus any modification of ϵ_{xx} or ϵ_{yy} do not impact the TE resonant behavior.

To sum up, the permittivity tensor used in the numerical simulations for out-of plane gelation sample under a transverse magnetic field (following z direction) is defined as follows:

$$\epsilon(M, \lambda) = \begin{pmatrix} \epsilon_{xx}(0) & i\epsilon_{xy}(M, \lambda) & 0 \\ -i\epsilon_{xy}(M, \lambda) & \epsilon_{yy}(0) & 0 \\ 0 & 0 & \epsilon_{zz}(M) = \epsilon_{zz}(0) + \Delta\epsilon_{zz} \end{pmatrix}. \quad (6)$$

Hence, as a first assumption, the TRE can be attributed to a magneto-induced anisotropy which can be related to the magnetostrictive property of the magnetic NPs. Indeed, Cobalt Ferrite is well known for its high magnetostrictive behavior; in other words a deformation of its crystal lattice occurs, under an applied magnetic field. Sukhorukov *et al* [31], have experimentally demonstrated a clear correlation between magnetostriction and magnetoreflexion in ferrimagnetic single crystal of CoFe_2O_4 . The influence of a magnetic field on the reflection spectra can be explained as follows: the application of a magnetic field results in a strong strain and deformation of the crystal lattice, which leads to a change in electron energy structure inducing a permittivity change of the MO material and hence a modification in the propagation constant of the guided modes. Referring to the grating coupling equation (4), this modification induces a spectral shift of the reflectance (or transmittance) resonance resulting in a resonant intensity modulation of the reflected (or transmitted) light.

We have to mention that this RE was also measured in transmission but it is smaller than in reflection geometry. It is the same for TMOKE for which the reflected spectrum relative shift is more important than the transmitted one [19].

To confirm this assumption, that the origin of the TRE is related to the NPs own behavior, we have plotted on figure 4(a) the intensity hysteresis loop of both TE and TM polarization for the in-plane gelation field device, i.e. $\vec{B}_{\text{gel}} // \vec{B}_{\text{meas}}$ (see figure 1(a3) and sample a3 in table 1.). Indeed, as demonstrated previously in [28], the coercive field (B_c) is maximum for a composite sample deposited under a gelation field with an orientation parallel to the measurement magnetic field. Hence, figure 4(a) illustrates the intensity loops in reflection for TE polarization at $\lambda = 1587$ nm (red curve) and for TM polarization at $\lambda = 1567$ nm (blue curve), for the structure of figure 1(a3) (sample a3). One should notice that for TM polarization intensity curve, we chose a wavelength where the TRE is too weak in order to have a pure TMOKE effect.

As seen in figure 4(a), the RE (pure TRE, red curve) presents a reciprocal hysteresis loop with a coercive field (B_c) that perfectly matches with that of the non-RE loop (TMOKE, blue curve). Indeed, the magnetization of ferrite cobalt NPs presents a hysteresis loop [32]. One can also mention that the TMOKE is linear in magnetization however the TRE is quadratic in magnetization. And since the magnetostriction

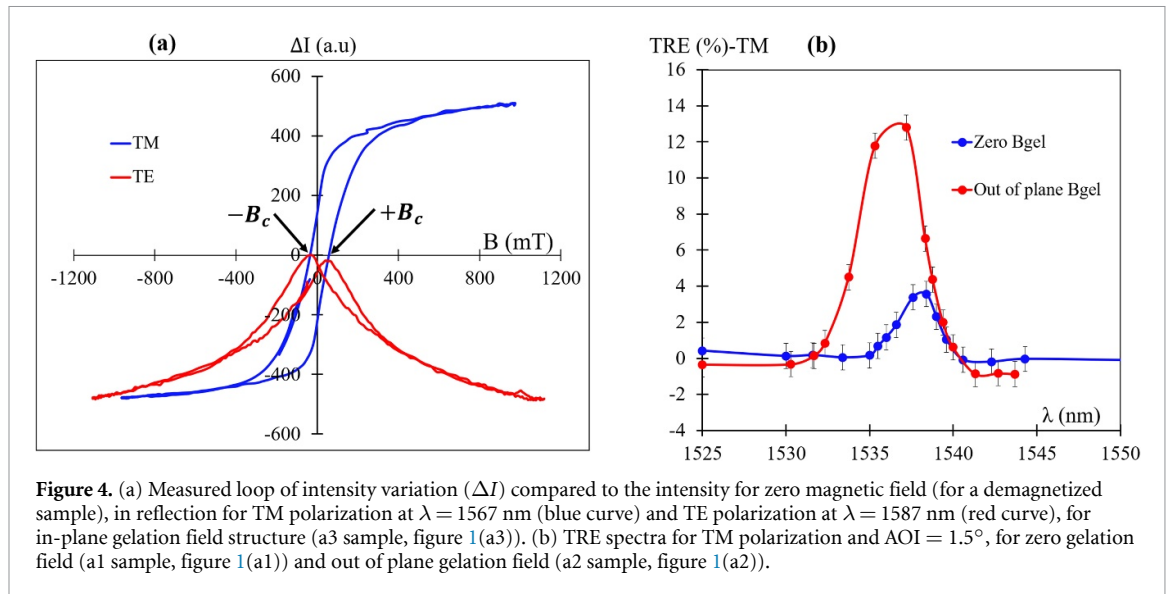


Figure 4. (a) Measured loop of intensity variation (ΔI) compared to the intensity for zero magnetic field (for a demagnetized sample), in reflection for TM polarization at $\lambda = 1567$ nm (blue curve) and TE polarization at $\lambda = 1587$ nm (red curve), for in-plane gelation field structure (a3 sample, figure 1(a3)). (b) TRE spectra for TM polarization and AOI = 1.5° , for zero gelation field (a1 sample, figure 1(a1)) and out of plane gelation field (a2 sample, figure 1(a2)).

effect is also quadratic in magnetization [31], we can confirm our hypothesis that this effect comes from the magnetostriction of the cobalt ferrite NPs.

To go further in the analysis, figure 4(b) illustrates the spectral behavior of TRE for two different samples with zero \vec{B}_{gel} (sample a1, figure 1(a1)) and out of plane \vec{B}_{gel} (sample a2, figure 1(a2)). As seen in this figure, the maximum TRE value for zero \vec{B}_{gel} sample (4%) is three times less than that of out of plane \vec{B}_{gel} sample (13%). Therefore, the anisotropy is higher when the NPs are all oriented in the same direction confirming our hypothesis that the demonstrated effect is related to oriented Cobalt Ferrite NPs. Indeed, in case of $\vec{B}_{\text{gel}} = \vec{0}$, all the NPs are randomly oriented in the sol-gel matrix. Hence, when a measurement magnetic field is applied the magneto-induced anisotropy axes have random directions and the total anisotropy is small. Whereas, in case of out-of plane \vec{B}_{gel} , all the NPs are aligned in the same direction and thus, all of them contribute to the magneto-induced anisotropy under applied magnetic field.

4. Conclusion

A novel kind of reciprocal magneto-optical effect was studied in this paper using an all-dielectric resonant grating patterned on a magnetic nanocomposite layer. This nanocomposite is made of magnetic NPs embedded in a silica matrix by sol gel process. This effect is defined as a reciprocal modification of the intensity of light under a transverse magnetic field. Contrary to the non-reciprocal TMOKE which exists only for TM polarization, TRE is present for both TM and TE. High values of 11% and 15% were demonstrated for TM and TE polarization respectively and for small angles of incidence. Such high values are not confirmed by RCWA numerical simulations that uniquely take into account, under magnetic field, the classical appearance of off-diagonal elements of the CoFe_2O_4 permittivity tensor. However, when a magneto-induced diagonal element is added, simulations are much more consistent with experimental values. Furthermore, TRE strongly depends on the NPs orientation inside the film.

In the first attempt to explain its origin, this effect is attributed to a magneto-induced anisotropy which can be related to the magnetostrictive property of the magnetic CoFe_2O_4 NPs.

Data availability statement

All data that support the findings of this study are included within the article (and any supplementary files).

ORCID iDs

Laure Bsawmaï  <https://orcid.org/0000-0003-3888-3673>

Emilie Gamet  <https://orcid.org/0000-0001-6524-5357>

François Royer  <https://orcid.org/0000-0002-0632-7915>

References

- [1] Aoshima K et al 2015 A magneto-optical spatial light modulator driven by spin transfer switching for 3D holography applications *J. Disp. Technol.* **11** 129–35
- [2] Sepúlveda B, Calle A, Lechuga L M and Armelles G 2006 Highly sensitive detection of biomolecules with the magneto-optic surface-plasmon-resonance sensor *Opt. Lett.* **31** 1085–7
- [3] Manera M G, Ferreiro-Vila E, Miguel Garcia-Martín J M, Garcia-Martín A and Rella R 2014 Enhanced antibody recognition with a magneto-optic surface plasmon resonance (MO-SPR) sensor *Biosens. Bioelectron.* **58** 114–20
- [4] Zvezdin A K and Kotov V A 1997 *Modern Magneto-optics and Magneto-optical Materials* (Philadelphia, PA: CRC Press)
- [5] Lutsenko S V, Kozhaev M A, Borovkova O V, Kalish A N, Temiryazev A G, Dagesyan S A, Berzhansky V N, Shaposhnikov A N, Kuzmichev A N and Belotelov V I 2021 Multiperiodic magnetoplasmonic gratings fabricated by the pulse force nanolithography *Opt. Lett.* **46** 4148–51
- [6] Chetvertukhin A V, Grunin A A, Baryshev A V, Dolgova T V, Uchida H, Inoue M and Fedyanin A A 2012 Magneto-optical Kerr effect enhancement at the Wood's anomaly in magnetoplasmonic crystals *J. Magn. Magn. Mater.* **324** 3516–8
- [7] Kudyshev Z A, Kildishev A V, Shalaev V M and Boltasseva A 2021 Machine learning-assisted global optimization of photonic devices *Nanophotonics* **10** 371–83
- [8] Pohl M et al 2013 Tuning of the transverse magneto-optical Kerr effect in magneto-plasmonic crystals *New J. Phys.* **15** 075024
- [9] Maksymov I S, Hutomo J and Kostylev M 2014 Transverse magneto-optical Kerr effect in subwavelength dielectric gratings *Opt. Express* **22** 8720–5
- [10] Fujita J, Levy M, Ahmad R U, Osgood R M, Randles M, Gutierrez C and Villareal R 1999 Observation of optical isolation based on nonreciprocal phase shift in a Mach-Zehnder interferometer *Appl. Phys. Lett.* **75** 998–1000
- [11] Kreilkamp L E, Belotelov V I, Yao Chin J Y, Neutzner S, Dregely D, Wehlius T, Akimov I A, Bayer M, Stritzker B and Giessen H 2013 Waveguide-plasmon polaritons enhance transverse magneto-optical Kerr effect *Phys. Rev. X* **3** 041019
- [12] Armelles G, Cebollada A, García-Martín A, García-Martín J M, González M U, González-Díaz J B, Ferreiro-Vila E and Torrado J F 2009 Magnetoplasmonic nanostructures: systems supporting both plasmonic and magnetic properties *J. Opt. A: Pure Appl. Opt.* **11** 114023
- [13] Ignatyeva D O, Knyazev G A, Kapralov P O, Dietler G, Sekatskii S K and Belotelov V I 2016 Magneto-optical plasmonic heterostructure with ultranarrow resonance for sensing applications *Sci. Rep.* **6** 28077
- [14] Caballero B, García-Martín A and Carlos Cuevas J C 2016 Hybrid magnetoplasmonic crystals boost the performance of nanohole arrays as plasmonic sensors *ACS Photonics* **3** 203–8
- [15] Belotelov V I, Bykov D A, Doskolovich L L, Kalish A N and Zvezdin A K 2009 Extraordinary transmission and giant magneto-optical transverse Kerr effect in plasmonic nanostructured films *J. Opt. Soc. Am. B* **26** 1594–8
- [16] Floess D, Chin J Y, Kawatani A, Dregely D, Habermeier H-U, Weiss T and Giessen H 2015 Tunable and switchable polarization rotation with non-reciprocal plasmonic thin films at designated wavelengths *Light Sci. Appl.* **4** e284–284
- [17] Royer Fçois, Varghese B, Gamet E, Neveu S, Jourlin Y and Jamon D 2020 Enhancement of both Faraday and Kerr effects with an all-dielectric grating based on a magneto-optical nanocomposite material *ACS Omega* **5** 2886–92
- [18] Bsawmaïi L, Gamet E, Royer F, Neveu S and Jamon D 2020 Longitudinal magneto-optical effect enhancement with high transmission through a 1D all-dielectric resonant guided mode grating *Opt. Express* **28** 8436–44
- [19] Bsawmaïi L, Gamet E, Neveu S, Jamon D and Royer Fçois 2022 Magnetic nanocomposite films with photo-patterned 1D grating on top enable giant magneto-optical intensity effects *Opt. Mater. Express* **12** 513
- [20] Belotelov V I, Bykov D A, Doskolovich L L, Kalish A N, Kotov V A and Zvezdin A K 2009 Giant magneto-optical orientational effect in plasmonic heterostructures *Opt. Lett.* **34** 398–400
- [21] Caicedo Roque J M, Arora S K, Ramos R, Shvets I V, Fontcuberta J and Herranz G 2010 Large magnetorefractive effect in magnetite *New J. Phys.* **12** 103023
- [22] Sukhorukov Y P, Telegin A V, Bebenin N G, Nosov A P, Bessonov V D and Buchkevich A A 2017 Strain-magneto-optics of a magnetostrictive ferrimagnet CoFe_2O_4 *Solid State Commun.* **263** 27–30
- [23] Krinchik G S and Artemjev V A 1968 Magneto-optic properties of nickel, iron and cobalt *J. Appl. Phys.* **39** 1276–8
- [24] Belotelov V I et al 2013 Plasmon-mediated magneto-optical transparency *Nat. Commun.* **4** 2128
- [25] Belotelov V I et al 2014 Magnetophotonic intensity effects in hybrid metal-dielectric structures *Phys. Rev. B* **89** 045118
- [26] Jamon D, Robert Sephane, Donatini F, Rousseau J J, Bovier C, Roux H, Serrughetti J, Cabuil Verie and Zins D 2001 Optical investigation of $\gamma\text{-Fe}_2\text{O}_3$ nanoparticle-doped silica gel matrix for birefringent components *IEEE Trans. Magn.* **37** 3803–6
- [27] Diwan E A, Royer F, Jamon D, Kekesi R, Neveu S, Blanc-Mignon M-F and Rousseau J 2016 Large spectral modification of the Faraday effect of 3D $\text{SiO}_2/\text{CoFe}_2\text{O}_4$ magneto-photonic crystals *J. Nanosci. Nanotechnol.* **16** 1–6
- [28] Bsawmaïi L, Jamon D, Gamet E, Neveu S and Royer F 2020 Enhanced magneto-optical response with a 1D resonant grating for sensing applications *Optical Sensing and Detection VI* (International Society for Optics and Photonics) vol 11354 p 113540Z
- [29] Rosenblatt D, Sharon A and Friesem A A 1997 Resonant grating waveguide structures *IEEE J. Quantum Electron.* **33** 2038–59
- [30] Wittekoek S, Popma T J A, Robertson J M and Bongers P F 1975 Magneto-optic spectra and the dielectric tensor elements of bismuth-substituted iron garnets at photon energies between 2.2–5.2 eV *Phys. Rev. B* **12** 2777–88
- [31] Sukhorukov Y, Telegin A, Bebenin N, Bessonov V, Naumov S, Shishkin D and Nosov A 2022 Strain-magneto-optics in single crystals of CoFe_2O_4 *Magnetochemistry* **8** 135
- [32] Choueikani F, Jamon D, Neveu S, Blanc-Mignon M-F, Lefkir Y and Royer F 2021 Self-biased magneto-optical films based on CoFe_2O_4 —silica nanocomposite *J. Appl. Phys.* **129** 023101